Waterborne Hyperbranched Polyurethane/Peptide Functionalized Carbon Dot Bio-nanocomposite

Highlight

The present chapter describes a combined bio-nano-macromolecular approach for bone tissue engineering. This approach relies on the properties of an ideal scaffold material with all the chemical cues required for fostering cellular growth and differentiation. Carbon dot prepared from corm of *Colocasia esculenta* was functionalized with four different peptides, *viz.* SVVYGLR, PRGDSGYRGDS, IPP and CGGKVGKACCVPTKLSPISVLYK by succinimide coupling method. These bio-nanohybrids were then used to fabricate tannic acid based waterborne hyperbranched polyurethane by using sound energy. This polymeric bio-nanocomposite was blended with 10% of gelatin and examined as a non-invasive delivery vehicle. *In vitro* assessment of the developed composite material revealed good osteoblast adhesion, proliferation and differentiation. Being guided by the panel of peptides, it exhibited *in vivo* ectopic bone formation ability. The studies on *in vivo* mineralization and vascularization revealed the occurrence of calcification and blood vessel formation. Thus, the study demonstrated suitability of hyperbranched waterborne polyurethane/peptide functionalized carbon dot bio-nanocomposite for accelerated bone tissue engineering application.

Parts of this chapter are published in

Gogoi, S., Maji, S., Mishra, D., Devi, K.S.P., Maiti, T.K., & Karak, N. Nano-bio engineered carbon dot-peptide functionalized water dispersible hyperbranched polyurethane for bone tissue regeneration, *Macromol. Biosci.* DOI: 10.1002/mabi.201600271 (In Press).

5.1. Introduction

The previous chapter (Chapter 4) explored the potentiality of waterborne hyperbranched polyurethane/carbon dot (WHPU/CD) nanocomposite for biomedical application. Profound cytocompatibility and tunable characteristics, like mechanical strength, microstructure, biodegradability, size and shape make it suitable for bone tissue engineering. However, despite of cytocompatibility, this synthetic material lacks target specific cell (bone tissue) recognition ability. This reduces its practical utility as a scaffold material. Therefore, improvement of bio-activity of WHPU/CD nanocomposite is necessary to use it in target specific *in vivo* bone tissue engineering application. This can be done by functionalizing the developed nanocomposite system with appropriate biomolecules like osteogenic peptides or proteins.[1,2] Many peptides are known to stimulate osteoblast adhesion, migration, proliferation and differentiation.[3-5]

Theoretically, the branches of a polymer could be conjugated with any kind of bio-active molecules including proteins and peptides. Generally, immobilization of biomolecule into polymer matrix is done by physical adsorption of the bio-motif onto the substrate surface or by the formation of chemical bonds between the biomolecule and substrate, either directly or through a spacer.[6] Formation of covalent chemical bonding seems promising for immobilization of biomolecules on polymer surface without causing any adverse effect on the bio-activity.[7,8] In this milieu, bio-nano fabrication of a biocompatible polymer can provide a unique proposition towards the development of an efficient scaffold material. Such an approach bestows upon the idea to prepare a stable bio-nanohybrid of peptides with multifunctional nanomaterial under mild condition and subsequent fabrication of the polymer matrix with the bio-nanohybrid by using green tool like ultra-sonication.

Thus, the present study proposed to use four different types of peptides, *viz.* SVVYGLR (SR-7, angiogenic peptide),[9] PRGDSGYRGDS (PS-11, cell adhesion peptide),[10] IPP (IP-3, osteoblast differentiating peptide)[11] and CGGKVGKACCVPTKLSPISVLYK (CK-23, osteogenic peptide)[12] to functionalize WHPU using CD as a nano-carrier. These are RGD sequenced peptides, which are the best known bio-motifs frequently employed for stimulating cell adhesion on synthetic surfaces. These four peptides were covalently conjugated with CD. These surface-

passivated bio-nanohybrids were used to fabricate WHPU using sound energy in an aqueous medium following an *ex situ* technique. Interaction of CD with polymer matrix through surface functional groups seems to eliminate the need of direct peptide/polymer functionalization, thus ensuring retention of osteogenic-activity of the bio-motifs in the polymer matrix. In this regard, CD appears as a suitable nanomaterial for peptide conjugation because of its profound bio-activity and capability to enhance osteoblast cell proliferation and differentiation as described in Chapter 4. This bio-nano-polymer composite was used as a non-invasive delivery scaffold after modifying with 10 wt% of gelatin. *In vitro* osteoblast cytocompatibility, proliferation and differentiation were studied in order to judge the aptness of the bio-nanocomposite as a scaffold material for bone tissue regeneration. Further, study on *in vivo* ectopic bone formation ability of the bio-nanocomposite was carried out to check its suitability as a non-invasive delivery vehicle. The work demonstrated improvement of biological properties of WHPU through an *ex situ* bio-nanofabrication technique.

5.2. Experimental

5.2.1. Materials

IPDI, PEG 600 and BD of similar grade and specifications were used as described in Sub-Chapter 2A (Section 2A.2.1.). Other chemicals including BMPA, TA, TEA and THF were used with similar grade and specifications as described in Sub-Chapter 2B (Section 2B.2.1.) for the preparation of WHPU. Gelatin from porcine skin Type A was procured from Sigma-Aldrich, USA and used to prepare WHPU/gelatin blend. CD was prepared from corm of *C. esculenta* as raw material as mentioned in Chapter 4 (Section 4.2.1.). Customized peptides, *viz.* SVVYGLR (SR-7), PRGDSGYRGDS (PS-11), IPP and CGGKVGKACCVPTKLSPISVLYK (CK-23) were purchased from GL Biochem Ltd., Shanghai, China. N-(3-dimethylaminopropyl)-N'-ethylcarbodiimide hydrochloride (EDC, Sigma-Aldrich, USA) and N-hydroxysulfosuccinimide (Sulfo-NHS, Pierce, USA) were used to functionalize the peptides with CD.

MG63 (human osteosarcoma) cell line was obtained from National Centre for Cell Science (NCCS), Pune, India. Cells were maintained in Dulbecco's Modified Eagle's Medium (DMEM, Hi-Media, India) supplemented with 10% Fetal Bovine

Serum (FBS, Life Technologies, USA) and penicillin streptomycin (1x, Sigma-Aldrich, USA) in a 5% CO_2 incubator at a temperature of 37 °C. 3-(4,5-dimethylthiazol-2-yl)-2,5-diphenyltetrazolium bromide (MTT) procured from Sigma, Germany was used to check the cellular viability of the bio-nanocomposite. Alamar Blue provided by Life Technologies, USA was used in the cell proliferation test. Alkaline phosphatase (ALP) assay kit purchased from Span Diagnostics, Surat, India was used to study osteoblast differentiation capability. 3,4-Dihydroxy-9,10-dioxo-2-anthracenesulfonic acid sodium salt (Alizarin Red S, Sigma-Aldrich, USA) was used in osteoblast differentiation study. Minimum Essential Medium-Alpha (α-MEM) used in various bio-tests was obtained from, Life Technologies, USA. β-Glycerophosphate disodium salt, ascorbic acid and dexamethasone were used as supplement in the medium used in *in vitro* osteoblast differentiation study. These bio-chemicals were procured from Sigma-Aldrich, USA. Collagenase type I enzyme purchased from Sigma-Aldrich, Germany was used in the *in vitro* biodegradation study. L-glutamine, 2-[4-(2-hydroxyethyl)piperazin-1-yl]ethanesulfonic acid (HEPES), ascorbate-2-phosphate and gentamycin sulfate used as supplement in murine osteoblast isolation study were obtained from Sigma-Aldrich, USA. RNA extraction kit (RNeasy Mini kit) provided by Qiagen, Germany was also used in the study. Hematoxylin and Eosin along with DPX mount obtained from Sigma-Aldrich, Germany were used for staining in histological study. FITC labelled anti-CD31 monoclonal antibody (Sigma-Aldrich, USA) was used for immunostaining in confocal microscopic vascularization study. Trypsin used in murine osteoblast isolation was procured from Hi-Media, India. Dulbecco's Phosphate-Buffered Saline (DPBS) and Phosphate Buffered Saline (PBS) were purchased from Sigma-Aldrich, USA. Other chemicals like alcohol, xylene and cell culture graded dimethyl sulphoxide (DMSO) were obtained from Hi-Media, India. Tissue culture polystyrene plate (TCPS, Hi-Media, India) was used as the control in the *in vitro* studies.

5.2.2. Characterization

UV-visible spectra of the bio-nanohybrids and bio-nanocomposite were recorded under same condition using the same photo-spectrometer as stated in Sub-Chapter 2B (Section 2B.2.2.). The shape and size of CD, as well as distribution of the bio-nanohybrid over the polymer matrix were visually studied by HRTEM analysis using

the same instrument as described in Chapter 4 (Section 4.2.2.). Probe type sonicator, Qsonica, Model: Q125, USA and bath sonicator, JSGW, India were used in the conjugation of CD and peptides. Percentage conjugation of peptides with CD was evaluated by using Reverse Phase High Pressure Liquid Chromatography (RP-HPLC), provided by Agilent Technologies, Model: 1260 Infinity, USA. The conjugated solutions of CD and peptides were analyzed on Zorbax 300SB-C18 column having dimension of 4.6 mm×250 mm. Multiskan Go, Thermoscientific, USA, multimode reader was used to record optical density of various samples at different wavelengths. Phase-contrast microscopes, Olympus, Model: CKX41, Japan, and Nikon, Model: H600L, Japan were used for imaging of the bio-samples. A confocal microscope, Olympus, Model: FV1000, Japan, was used in the vascularization study.

5.2.3. Methods

5.2.3.1. Preparation of WHPU

WHPU was prepared by following a pre-polymerization technique as described in Sub-Chapter 2B (Section 2B.2.3.1.). 10 wt% of TA was used as bio-based raw material.

5.2.3.2. Preparation of CD

CD was prepared by using corms of *C. esculenta* as raw material as described in Chapter 4 (Section 4.2.3.1.).

5.2.3.3. Conjugation of CD with peptides

CD and peptides were conjugated by succinimide coupling method (EDC/sulpho-NHS coupling).[13] Briefly, CD solution (100 μg mL^{-1}) was sonicated in an ice bath using a probe type sonicator under a power of 40 W for 1 h. Then, 5 mM of Sulfo-NHS and 1 mM of EDC were added into the CD solution and the mixture was bath sonicated for 1 h. Thereafter, 1 mM of each peptide was added to the CD solution separately and stirred vigorously for overnight in an ice bath. The bio-nanohybrids of CD and peptide thus obtained were stored at 4 °C and coded as CDP. The percentage of conjugation between CD and peptides was determined by RP-HPLC analysis. A graded mixture of acetonitrile and water (10-90%) was used for RP-HPLC study at a flow rate of 1mL min^{-1}. Pure peptide and CD solutions were taken as the standards for quantification.

5.2.3.4. Bio-nano fabrication of WHPU

Conjugated CDPs (1 wt% of total solid content) were added to the aqueous dispersion of WHPU and mixed well by stirring. The ratio of CDPs in the polymer was maintained according to CD/peptide percentage conjugation, so that all the four peptides were present in equal amount. Accordingly, a ratio of CK23 : PS11 : SR7 : IP3 = 1 : 1.16 : 1.44 : 2.69 was maintained. This WHPU/CDP polymeric solution was mixed with 10% gelatin in the ratio of 10:1 and the solution was stirred for 1 h followed by bath sonication for 10 min in an ice cool condition. The developed CDP fabricated WHPU was coded as CDP-*f*-PU.

5.2.3.5. In vitro cell adhesion

An indirect cell counting method was employed for osteoblast adhesion test on the tested polymeric systems.[14] 1×10^5 MG63 cells were seeded onto the polymeric materials coated plates (96 wells), which include WHPU, WHPU/gelatin and CDP-*f*-PU. For each polymer, experiment was performed in triplicate. Similar number of cells was also seeded onto TCPS plate, which served as the control. The plates were incubated for different time intervals, wherein un-adhered cells were collected and counted under phase-contrast microscope with the help of a Neuber's hemocytometer. The number of un-adhered cells was subtracted from the original number of seeded cells in order to obtain the number of adhered cells using the following formula:

$$N_{\text{Adhered cell}} = N_{\text{Seeded cell}} - N_{\text{Unadhered cell}} \ldots\ldots\ldots\ldots\ldots\ldots (\mathbf{Eq.\,5.1})$$

5.2.3.6. In vitro proliferation

MG63 human osteoblast cell line was used for *in vitro* osteoblast cell proliferation study on the polymeric substrates (WHPU, WHPU/gelatin and CDP-*f*-PU) by following Alamar Blue assay.[14] 20 µL (containing 1×10^4 cells) of MG63 cell suspension was applied on the polymer coated 96 well plate and control well (TCPS). These plates were incubated in 5% CO_2 incubator at 37 °C with complete DMEM comprising of 10% FBS. The incubation was continued for 7 days with medium changed on every alternate day. For Alamar Blue assay, the working solution was prepared by adding 10% of Alamar Blue in incomplete DMEM (without FBS) separately and this working solution was added to the cells by replacing the old

medium followed by incubation at 37 °C in a 5% CO_2 incubator for 4 h. After incubation, culture supernatants were collected and OD values were recorded at 570 nm and 600 nm. The calculations were carried out according to the manufacturer's instruction (Sigma-Aldrich, USA).

5.2.3.7. In vitro osteoblast differentiation

The osteoblast cell differentiation study was conducted by alkaline phosphatase (ALP) assay.[15] 20 µL (containing 2×10^4 cells) of MG63 cell suspension was seeded to different polymer coated (WHPU, WHPU/gelatin and CDP-*f*-PU) 96 well plate and control well (TCPS). These were then incubated in a humidified incubator (37 °C, 5% CO_2) with differentiating medium comprising of DMEM supplemented with 10% FBS, sodium-β-glycerol phosphate (10 mM), ascorbic acid (50 µg mL^{-1}) and dexamethasone (100 mM). Osteoblast differentiation was determined on the 3rd, 6th and 9th day of the test. The medium was collected from the wells and the ALP activity was determined according to the manufacturer's instruction using ALP assay kit. Total protein content of the media was determined by following Bradford assay and was done according to the manufacturer's instruction (Sigma, USA).

5.2.3.8. In vitro biodegradation

The biodegradation analysis was carried out by measuring the change in the sample weight over time under simulated physiological conditions.[16] Collagenase type I enzyme was used for *in vitro* biodegradation study. PBS (pH 7.4) containing the enzyme system at a concentration of 0.1% (v/v) was poured onto 500 mg of the tested materials separately. After every 3 days, PBS was removed, polymers were soaked in tissue, air dried and weighed. The change in their weight was calculated as a function of time. The percentage degradation was evaluated according to the following equation:

$$\%\text{Degradation} = \frac{W_{\text{Initial}} - W_{\text{Final}}}{W_{\text{Initial}}} \times 100 \ldots\ldots\ldots\ldots\ldots\ldots\ldots (\mathbf{Eq.\ 5.2})$$

where, W_{Initial} and W_{Final} represent the initial and final dry weight of the polymeric materials, respectively.

5.2.3.9. Animal

The male Swiss albino mice of 3-4 weeks old and weighing 25-27 g were acquired from the Animal House, Department of Biotechnology, Indian Institute of Technology Kharagpur, India. The animals were kept properly at temperature of 22-26 °C, relative humidity of 72% with strict maintenance of 12 h of light and dark cycles and given sufficient nutrition and water ab libitum. All animal experimental protocols were performed with due approval of the Animal Ethical Committee, Indian Institute of Technology, Kharagpur (Ref. No.764/03/ac/CPCSEA).

5.2.3.10. Isolation of murine osteoblast and characterization

Murine osteoblast was isolated by enzymatic digestion of calvariae of neonatal mice.[17] 3-4 days old neonatal mice were euthanized *via* chloroform over anesthesia. The pubs were surface sterilized by submerging them in 70% ethanol for few minutes. Calvariae portions of the skull containing parietal and frontal bone pairs were dissected out and collected in cold DPBS under a sterile environment. The separated calvariae were chopped into 1 mm^2 pieces, which were digested enzymatically using 0.3% trypsin and 0.4% collagenase for 15 min at 37 °C with continuous agitation. The cells obtained out of each digestion were collected in complete medium. The digestates of 3^{rd} to 5^{th} digestion were pooled together, filtered *via* 70 µm cell stainer and centrifuged at 250×g to obtain a cell pellet. The cell pellet thus obtained was re-suspended in complete α-MEM supplemented with 4 mM L-glutamine, 25 mM HEPES, 100 µM ascorbate-2-phosphate, 50 µg mL^{-1} gentamycin sulfate and 10% FBS. The cell suspension was seeded in a T-25 culture flask and cultured in an incubator at 37 °C with 5% CO_2 with frequent change of media. Characterization of primary osteoblast obtained from the enzymatic digestion of murine calveriae was done by reverse transcription polymerase chain reaction (RT-PCR) based detection of markers. Total RNA was isolated using RNA extraction kit (Qiagen RNeasy Mini kit) and the cDNA synthesis was carried out according to the manufacturer's instruction (Bio-Bharti, MuLV Reverse Transcriptase Plus Kit, India). Amplification of genes was done by using PCR reaction with four sets of gene specific primers (Osteocalcin, ScaI, ALP, RunX2 and a house keeping gene GAPDH). The primer sequences included for the amplification were 5' GCAATAAGGTAGTGAACAGACTCC 3' (Osteocalcin_F), 5' AGCAGGGTTAAGCTCACACTG

3‘ (Osteocalcin_R), 5’CTCTGAGGATGGACACTTCT 3‘ (ScaI_F), 5‘ GGTCTGCAGGAGGACTGAGC 3‘ (ScaI_R), 5’ CGGCCCTCCCTGAACTCT 3‘ (RunX2_F), 5‘TGCCTGCCTGGGATCTGT 3’ (RunX2_R), 5’ CCAACTCTTTTGTGCCAGAGA 3’ (ALP_F), 5’ GGCTACATTGGTGTTGAGCTTTT 3‘ (ALP_R), 5’AGGTCGGTGTGAACGGATTTG 3‘ (GAPDH_F), 5’ TGTAGACCATGTAGTTGAGGTCA 3‘ (GAPDH_R). The PCR products were verified *via* agarose gel electrophoresis. The isolated murine osteoblast was further characterized for its mineralization capability by staining the cells with Alizarin Red S. The cells were fixed and exposed with 1mg mL^{-1} staining solution of Alizarin Red S followed by imaging under a phase-contrast microscope.

5.2.3.11. In vivo ectopic bone formation

Ectopic bone formation study was conducted to access the *in vivo* osteogenic capability of CDP-*f*-PU, which was implanted non-invasively in different inbred mice. Two variants of the selected polymeric gel formulation were considered for *in vivo* injection, i.e. CDP-*f*-PU (without murine osteoblast) and CDP-*f*-PU (with murine osteoblast). In CDP-*f*-PU (with osteoblasts), 5×10^5 isolated murine osteoblasts (re-suspended in 100 µL of DEME media) were added per mL of CDP-*f*-PU. 0.3 mL each of the two variants was aseptically injected subcutaneously *via* 16 gauge needles in different inbred mice (Swiss albino, male, 3-4 week age) near the dorsal region. In addition, each type of injection was made in five animals. The animals were maintained for 2 weeks with ample quantity of food and water. After the period, the animals were sacrificed and the injectates were retrieved for analysis.

5.2.3.12. Histochemistry

The retrieved injectates were fixed by using neutral buffered formalin for 48 h with continuous agitation followed by profuse washing in tap water. The samples were further dehydrated by using graded alcohols and the completely dehydrated samples were embedded in molten paraffin. The paraffin was cooled to room temperature and trimmed to partially expose the samples. The trimmed paraffin blocks were mounted on a rotary microtome and thin slices (5 µm) were cut out from the samples. These slices were mounted over APTES coated glass slides with the help of a tissue floatation bath. The slices were dewaxed and rehydrated using xylene and graded alcohols, respectively. To ensure a firm bonding between the tissue slices and glass surface, the slides were treated with warm Bouin’s fluid for 15 min. The slides were

then stained with Hematoxylin and Eosin. After staining, the glass slides were dehydrated through graded alcohols and glass coverslips were mounted on the tissue slices using DPX mountant. The tissue sections were analyzed under microscope in the next day.

5.2.3.13. Mineralization

The histological glass slides prepared from the method described previously were used for the study of mineralization on the explant retrieved. In order to visualize mineralized nodules, the glass slides were stained with Alizarin Red S. Briefly, the fixed cells were exposed to a staining solution containing 1mg mL^{-1} of Alizarin Red S in distilled water.[18] The pH was adjusted to 5.5 with dilute ammonium hydroxide. After 15 min, the staining solution was thoroughly washed with distilled water followed by imaging under a microscope.

5.2.3.14. Confocal microscopic vascularization

Confocal microscopic imaging was performed to observe the vascularization pattern in the harvested explants. The explants fixed in histological slides were de-paraffinized by using xylene and rehydrated by using graded alcohols (100%-50%) and distilled water, respectively. Antigen retrieval was done by treating the section with pre-warmed sodium citrate buffer for 20 min followed by washing with PBS. The sections were then subjected to immunostaining with FITC labelled anti-CD31 monoclonal antibody (Dakocytomation). The immunostained samples were sufficiently washed with PBS and then analyzed by a confocal microscope.

5.2.3.15. In vivo toxicity analysis

The polymeric gel of CDP-*f*-PU with and without osteoblasts (five in each group) were prepared and injected into the peritoneal cavity of the mice. The animals were weighed prior to the experiments and blood parameters were evaluated before the administration by collecting the blood from mice tail. The normal behavior and food habits were monitored throughout until the end of the experiment. On the 14^{th} day, the mice were sacrificed and the weight of the organs was taken. Blood was collected by puncturing the heart and collected in K3 EDTA tubes. All the tests were conducted according to the manufacturer's instruction (Span Diagnostics, Ahmedabad, India). On the other hand, detail biochemical analysis was done for serum glutamic pyruvic

transaminase (SGPT), serum glutamic oxaloacetic transaminase (SGOT), ALP, urea and glucose. The test was done according to the manufacturer's instruction (Span diagnostics, Ahmedabad, India).

5.2.3.16. Statistical analysis

Data obtained were analyzed and plotted in MS Excel (Office 2010, Microsoft) and Origin 8.5 (OriginLabs). Curve fitting simulations were performed in MS Excel. Each experiment was done in triplicates and values were presented as mean±SD. In addition, Student's t-test function of MS Excel was used to deduce statistical significance of the data. Data with p value <0.05 were considered as significant.

5.3. Results and Discussion

5.3.1. Material preparation and characterization

5.3.1.1. Conjugation of CD/peptide

The formation of CD was confirmed by TEM analysis. It possessed spherical morphology with average size of 3.4 nm, size distribution of 2.2-5.8 nm and layer spacing of 0.341 nm as shown in **Figure 5.1a-d**. UV-visible spectrum showed an absorption peak at wavelength 265 nm (**Figure 5.2a**), which confirmed formation of CD. Raman spectrum of CD demonstrated two bands, *viz.* D and G bands at 1365 cm^{-1} and 1584 cm^{-1}, respectively which further ensured the formation of CD as discussed in Chapter 4 (Section 4.3.2.) (**Figure 5.2b**). Covalent conjugation of peptides with CD

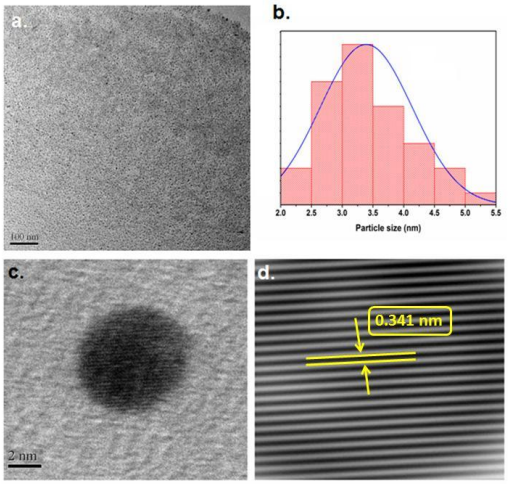

Figure 5.1. (a) TEM image of CD, **(b)** Size distribution of CD, **(c)** HRTEM image of CD and **(d)** IFFT of HRTEM of CD.

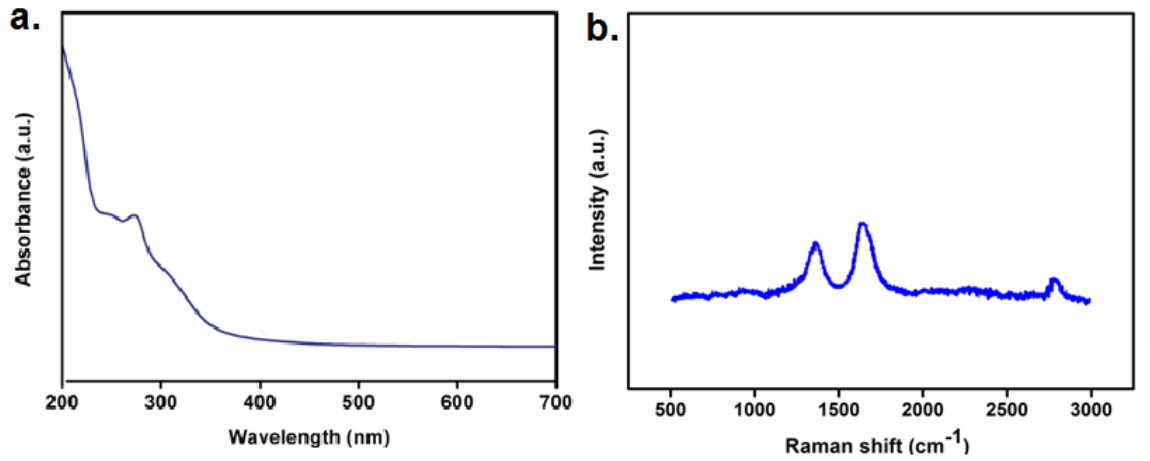

Figure 5.2. (a) Raman spectrum and **(b)** UV-visible spectrum of CD.

was carried out by carbodimide method (EDC/sulpho-NHS coupling).[19] CD with various forms of surface passivation contains a large number of functional groups, which facilitate excellent aqueous solubility and provide potential sites for its ready modification or functionalization with other organic molecules. Among the various functional groups, -COOH acted as the active site for peptide conjugation (**Scheme 5.1**). The percentage conjugation between CD and peptides was analyzed by RP-HPLC. The chromatographic profiles exhibited two different peaks for CDPs (**Figure 5.3**). The second peak in the chromatographic profiles is attributed to the presence of conjugated peptides. Here the absorbance was monitored at 220 nm (absorption wavelength of amino acids). The RP-HPLC result showed more than 30% conjugation

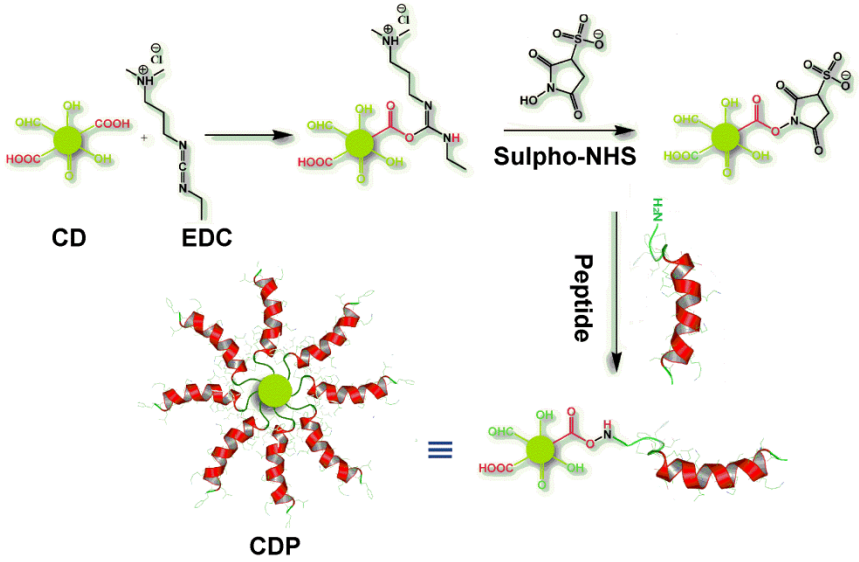

Scheme 5.1. Schematic presentation of functionalization of CD and peptides.

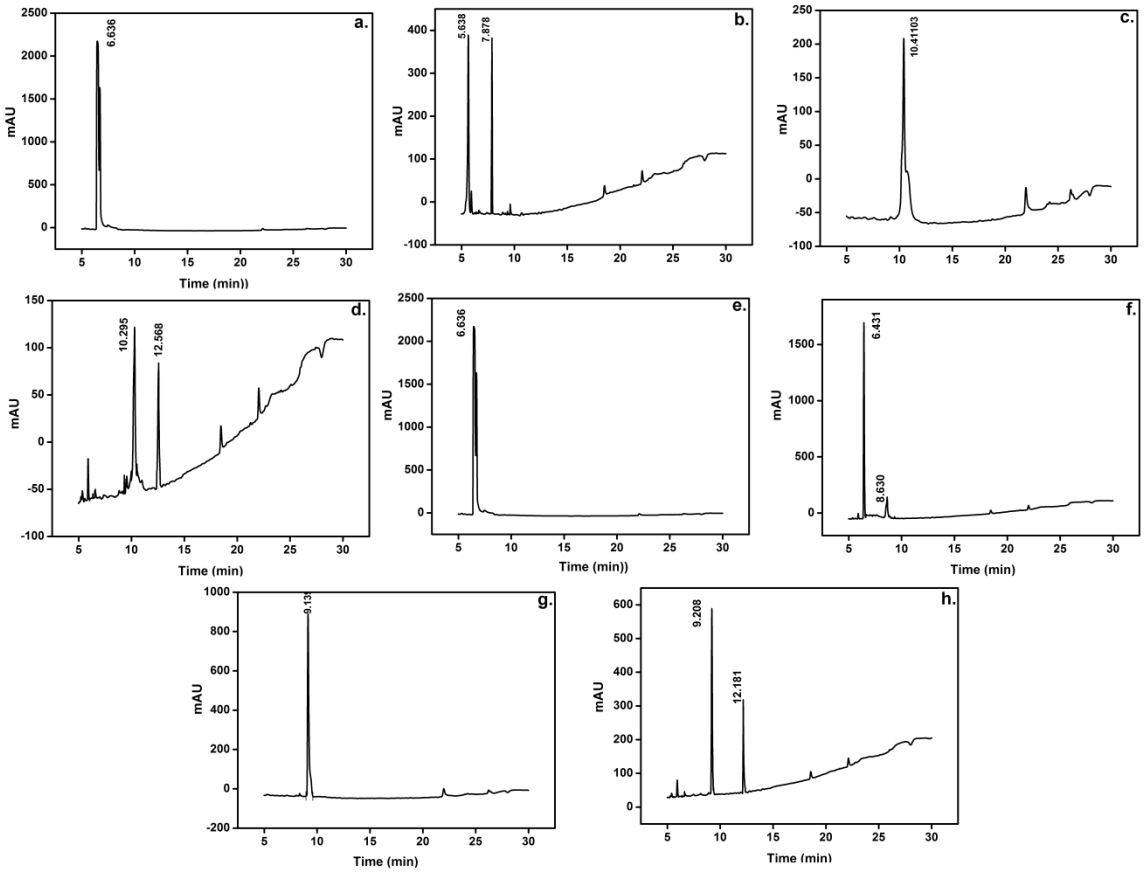

Figure 5.3. RP-HPLC profiles of **(a)** peptide PS11, **(b)** PS11 conjugated with CD, **(c)** peptide CK23, **(d)** CK23 conjugated with CD, **(e)** peptide IP3, **(f)** IP3 conjugated with CD, **(g)** peptide SR7 and **(h)** SR7 conjugated with CD.

of CK23 and PS11 peptides with CD. Conjugation percentage was found low for the peptide IP3 (**Figure 5.4b**). This is probably because of the fact that peptide IP3 consists of only three amino acids and has low number of amino groups, which reduces the chances of succinimide coupling between peptide and CD. UV-visible spectra of CDPs revealed two absorption peaks at wavelength 265 nm ascribed to CD and 340 nm for the peptide moiety (**Figure 5.4a**). This further confirmed successful conjugation of peptides with CD.

5.3.1.2. Bio-nanofabrication of WHPU

Bridging of a stable link between a polymer and peptides without affecting bioactivity of the later is the prerequisite for successful bio-functionalization of any polymeric biomaterial.[20] The current study utilized a simple technique, which relies on aqueous phase bio-fabrication of WHPU. WHPU was fabricated by an *ex situ* technique using

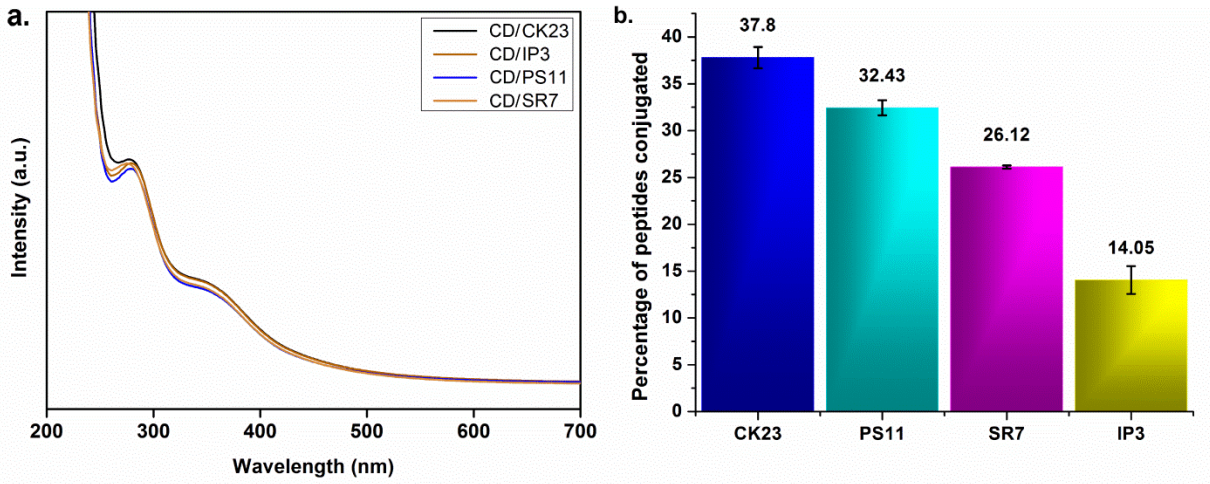

Figure 5.4. (a) UV-visible spectra of CDP and **(b)** Percentage conjugation of peptides with CD.

sound energy. Here it is pertinent to mention that aqueous solubility of both the polymer and bio-nanohybrid is significant to achieve a uniform sharing of CDPs over the WHPU matrix. Multifunctional CD provided a strong interfacial interaction with the polymer matrix through different chemical functionalities (**Scheme 5.2**). This further aided homogeneous mixing of the bio-nanohybrid in WHPU. The TEM image of CDP-*f*-PU as depicted in **Figure 5.5a** confirmed the fact. UV-visible spectrum showed a doublet around 280 nm region and another peak at 360 nm (**Figure 5.5b**). Deconvolution of the former revealed existence of two peaks; weakly intense absorption at wavelength 265 nm is attributed to CD, while strongly intense peak at

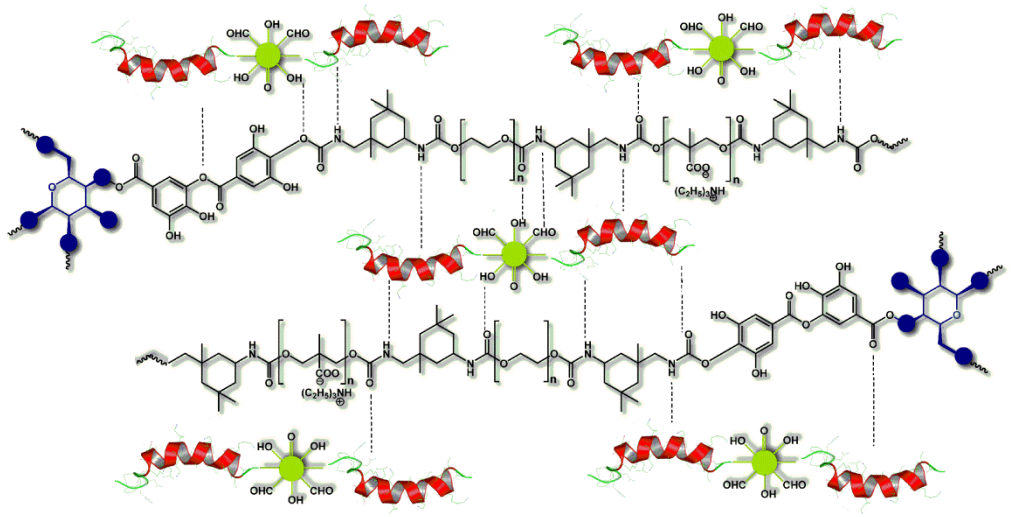

Scheme 5.2. Schematic presentation of *ex situ* fabricated CDP-*f*-PU.

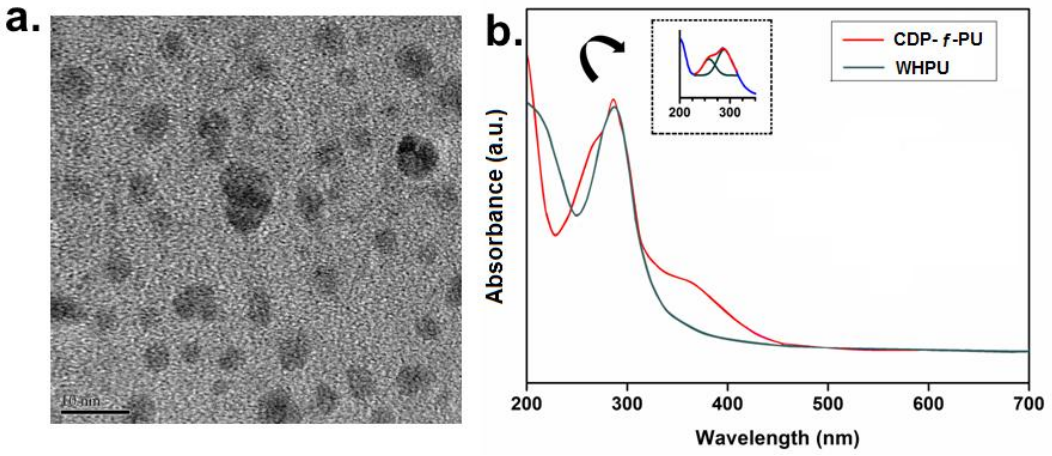

Figure 5.5. (a) TEM image of CDP-*f*-PU matrix (scale bar represents 10 nm) and **(b)** UV-visible spectra of CDP-*f*-PU and WHPU.

wavelength 280 nm is assigned to the catechol fraction of WHPU. The other absorption peak at wavelength 360 nm is ascribed for the peptide moieties. To ensure the stability of the whole composite system, it was kept under stimulated body fluid for 72 h and then UV-visible spectrum of the supernatant was taken. However, no peak of CD or peptide was observed, which indicates formation of a stable bio-nanocomposite system.

5.3.2. *In vitro* biological study

5.3.2.1. Cytocompatibility

Cytocompatibility study of CD with MG63 cell line confirmed its suitability as a nano-carrier for osteogenic peptides. The study showed cytocompatibility of CD at different concentrations after 24 and 48 h (**Figure 5.6**). The results revealed more than 90% of cell viability at a CD concentration of 25 μg mL^{-1} for both the time periods. From the data it appeared that viability is comparatively less (below 70%) at high concentration (100 μg mL^{-1}) for 24 h. However, for *in vivo* experiment very low concentration of CD was used (1 μg mL^{-1}). At this concentration CD showed viability of 95% (for both 12 and 24 h) with MG63 cells. Hence, CD can be said to be biocompatible for the present study. The comparative cytocompatibility study of WHPU, WHPU/Gelatin and CDP-*f*-PU was also performed. The bar graph shows MG63 cell viability in percentage against the tested samples and control (**Figure 5.7a**). WHPU showed a low cell viability of 25% as compared to the control (considering 100% cell viability for TCPS control). However, after blending with gelatin, the

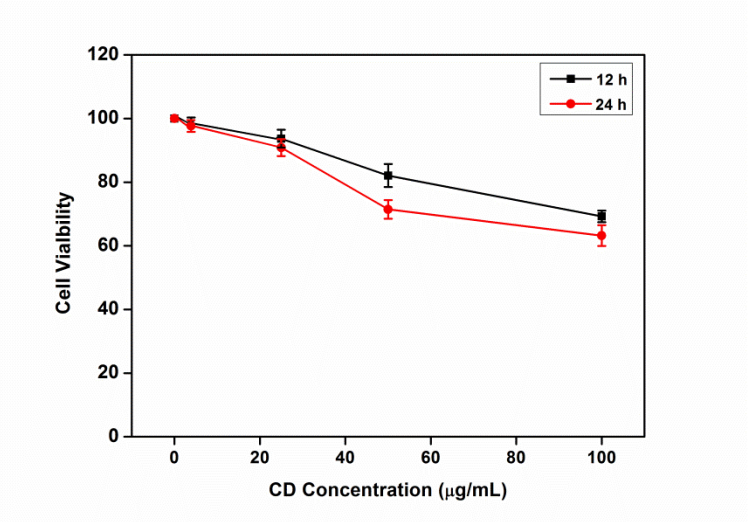

Figure 5.6. MG63 cell viability assay against different concentrations of CD after 12 and 24 h.

compatibility of WHPU towards MG63 cells increased up to 80%. On the other hand, CDP-*f*-PU exhibited exceptional cytocompatibility of 105% compared to the control. Thus, the study shows an excellent biocompatibility of CDP-*f*-PU. Increase in cytocompatibility is most certainly due to the presence of CD conjugated osteogenic peptides as well as other cell adhesion and proliferation peptides, which enhanced the osteoblast viability of WHPU after functionalization.

5.3.2.2. Cell adhesion

Osteoblast cell adhesion test confirmed suitability of the bio-nanocomposite for MG63 cell adhesion on its surface. The study revealed that the threshold cellular adhesion time was reached after 4 h for all the tested polymeric materials (**Figure 5.7b**). However, the degree of adhesion was found to be different on different materials. With an initial seeding of 1×10^5 cells, the control showed an adherence of 90% (9×10^4 cells) after 4 h. Osteoblasts adherence on WHPU coated wells was 65% and 70% after 4 h and 8 h, respectively. When WHPU was blended with biopolymer gelatin, cell adhesion increased up to 85-90% at the end of 4^{th} h. After coating the wells with CDP-*f*-PU, the osteoblast adhesion reached 95%. The increment of cell adherence on CDP-*f*-PU can be attributed to the presence of adhesion peptides, which possess RGD sequence. This sequence is well known as a key binding sequence for cell attachment, specifically working with integrin.[21] Additionally, biopolymer gelatin also possesses RGD sequence, which also contributed towards enhanced osteoblast

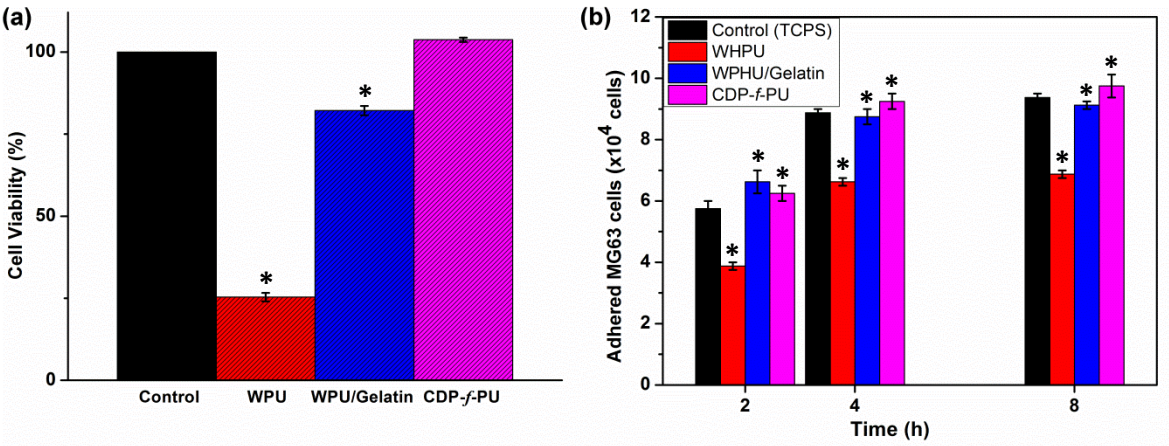

Figure 5.7. (a) MTT cell viability assay and **(b)** Number of MG63 cells adhered *versus* time (h) on control, WHPU, WHPU/Gelatin and CDP-*f*-PU. Values are presented as mean±SD of three different observations and significance level was evaluated by comparing with the control using student t-test statistics: *P<0.05.

adhesion.[22] Adhesion of cell is considered as one of the first phases of cell-material interaction, which determines the cell's capability of proliferation, migration and differentiation.

5.3.2.3. Cell proliferation

In vitro proliferation of osteoblast was carried out by Alamar Blue assay and the proliferation rate was calculated as the percentage of Alamar Blue reduction. There exists a direct relationship between proliferation rate and Alamar Blue reduction values.[23] According to the osteoblast proliferation study, a constant increase in the proliferation rate was witnessed till day 7. There after a steady rate of proliferation was recorded (**Figure 5.8**). This might arise due to the confluent nature of the cells, which resulted in stagnancy of cell proliferation. However, when we compared the results of three different tested materials against the control, we found CDP-*f*-PU as the best material for MG63 proliferation. It was found that at the end of day 7, CDP-*f*-PU exhibited greater than 90% of Alamar Blue reduction, which was even more than that of the control. WHPU showed the lowest proliferation rate of 55% after day 7. Upon blending with gelatin the proliferation of MG63 increased up to 80%. Clearly, the results indicate that biopolymer gelatin had augmenting the cell proliferation rate, which was further enhanced on functionalization of WHPU with the multiple peptides.

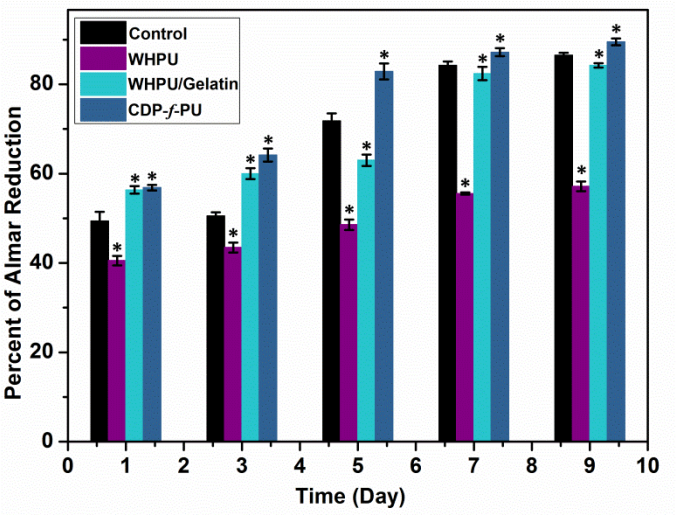

Figure 5.8. Alamar Blue cell proliferation assay of MG63 cells on control, WHPU, WHPU/Gelatin and CDP-*f*-PU. Values are presented as mean±SD of three different observations and significance level was evaluated by comparing with the control using student t-test statistics: *P<0.05.

5.3.2.4. Osteoblast differentiation

In vitro ALP activity on treated MG63 cells suggested that the probable osteoblast differentiation potency of CDP-*f*-PU is better than that of WHPU and WHPU/gelatin blend. In each case, the threshold enzyme activity was attained after 20 days of cell seeding as shown in **Figure 5.9**. CDP-*f*-PU showed the maximum ALP activity (35

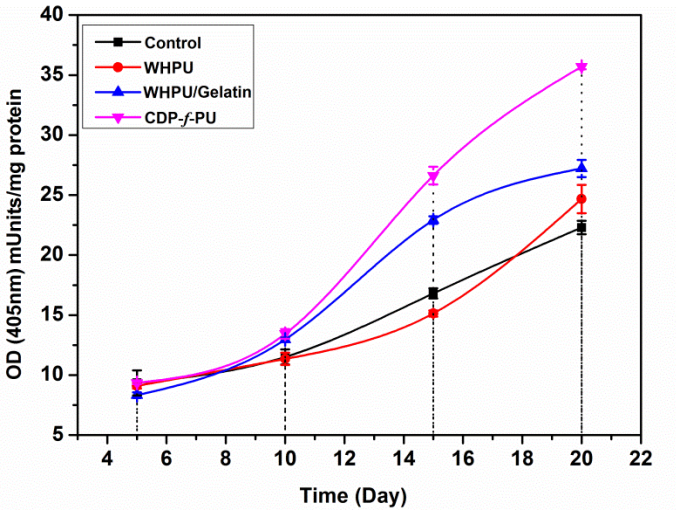

Figure 5.9. Cell differentiation of MG63 cells on control, WHPU, WHPU/Gelatin and CDP-*f*-PU as investigated by ALP assay. Values are presented as mean±SD of three different observations.

mUnit mg^{-1} of protein). Initially on 5th day, similar level of ALP activity was shown by MG63 cells seeded on different polymeric materials. The change in the enzyme activity was noted from day 10 onwards. There was a constant increase of enzyme activity in case of WHPU and control, whereas for CDP-*f*-PU the enhancement was double folded (on day 10, activity was 13.43 mUnit mg^{-1} of protein and on day 15 activity was 26.62 mUnit mg^{-1} of protein). The gradual increase in ALP activity was due to the initial acclimatization of MG63 cells with the polymeric materials to adhere and proliferate. This was followed by differentiation of the cells. The study showed that modification of WHPU with CD conjugated differentiation peptides (IPP) enhanced bone differentiation ability of the bio-nanocomposite significantly.[24]

5.3.2.5. Biodegradation

For any scaffold material, the rate of biodegradation is considered as an important factor. Degradation of the polymeric scaffold in a given period of time under controlled mechanism eliminates the necessity of surgical invasion. The degradation study was carried out by incubating the developed material with a solution of 0.1% collagenase enzyme (v/v) as stated in the experimental section. Collagenase specifically cleaves collagen/gelatin fibrils at Gly775–Leu/Ile776, located in the region with a loose triple helical conformation. From the results, significant variation in the degradation profiles of WHPU, WHPU/gelatin blend and CDP-*f*-PU was observed (**Figure 5.10**). Among the three systems, WHPU/gelatin blend showed the maximum rate of degradation, where almost ~67% of the polymer was degraded after 24 days. On the other hand, degradation percentage of CDP-*f*-PU was comparatively slower, which revealed ~60% weight loss during the experimental period. WHPU showed the slowest percentage of degradation (~44%) at the end of the analysis. The high percentage of degradation of WHPU/gelatin blend might be due to the presence of biopolymer gelatin, which is a known substrate of collagenase enzyme.[25] In the absence of gelatin, the degradation of WHPU decreased more than 50%. The degradation rate of CDP-*f*-PU was comparatively slower compared to WHPU/gelatin due to the physical interactions between the peptide conjugated CD and gelatin, which prevented the exposure of collagenase specific cleavage site of gelatin, thus reducing the degradation rate. The reduced rate of polymer degradation would assist in proper bone wound healing process.

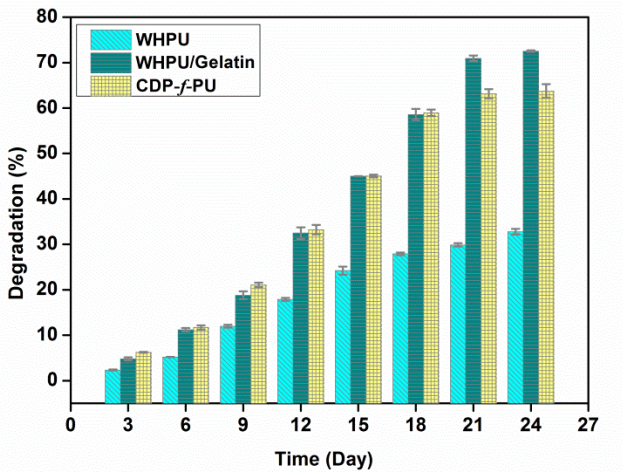

Figure 5.10. Degradation percentages of WHPU, WHPU/Gelatin and CDP-*f*-PU against collagenase. Values are presented as mean±SD of three different observations.

5.3.3. *In vivo* biological study

5.3.3.1. CDP-f-PU as non-invasive delivery vehicle

Study on *in vivo* polymer stability was conducted before *in vivo* osteogenic assessment. *In vivo* stability of the injectable *in situ* polymer is especially important for bone tissue engineering application. In the present study, the injected polymeric gel formulations were successfully retrieved after 24 h of implantation from the injectate position of the euthanized mice. The study revealed no apparent signs of inflammation, e.g. redness or edema at the site of implantation, which implied that these polymeric gels are non-immunogenic in nature. Considering the osteogenic behavior, *in vitro* results and *in vivo* polymer gel stability, CDP-*f*-PU was selected as the polymeric composition for subsequent ectopic bone formation study in two different compositions: (i) without osteoblast cells and (ii) with osteoblast cells. However, WHPU was not considered for *in vivo* study as it exhibited very poor *in vitro* performance (compared to control). *In vivo* stability of both the compositions of CDP-*f*-PU retrieved after 14 days of implantation was shown in **Figure 5.11**.

5.3.3.2. Isolation of murine osteoblast and characterization

The primary murine osteoblasts were isolated from calvariae of neonatal mice as described in the experimental section. The cells obtained from pool of 3rd-5th digestate showed a cubical flattened morphology, which is one of the characteristic features of primary osteoblast. The osteoblasts shown in **Figure 5.12a** are after the

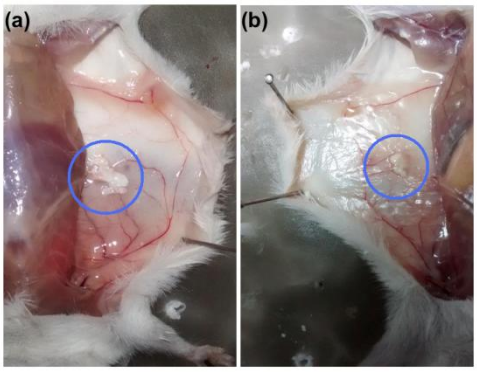

Figure 5.11. Representative macroscopic images of post-mortal mouse showing the location and texture of **(a)** CDP-*f*-PU (with osteoblasts) and **(b)** CDP-*f*-PU (without osteoblasts) after 14 days of post-implantation.

first passage. The isolated cells were characterized for the presence of osteoblastic markers through RT-PCR based study. The result indicates that the cells were positive marker for osteocalcin, RunX2, Sca1 and ALP (**Figure 5.12d**). Moreover, the expression levels of osteocalcin and RunX2 were higher than Sca1 and ALP. Presence of high quantity of osteocalcin and RunX2 indicates that isolated cells from calvariae were osteoblast in nature.[26,27] Whereas, low level expression of ALP and Sca1 confirms that the isolated cells were fully differentiated osteoblasts and free from the presence of early stage precursor osteoblast lineage.[28,29] The cells obtained from the pool of 3rd-5th digestate were re-characterized in terms of their matrix mineralization ability (**Figure 5.12b** and **c**) by staining with Alizarin Red S. The cells showed significant Alizarin Red S staining after 5th days of culture. The result indicates that the isolated cells were indeed bone cells and not contaminated by other type of cells.

5.3.3.3. Ectopic bone formation

Following primary murine osteoblast isolation, two compositions of CDP-*f*-PU (with and without primary osteoblasts) were subcutaneously injected in an ectopic region of the mice. After two weeks, the bio-nanocomposite gels with both compositions were retrieved. The retrieved systems were bony white in color and gelatinous soft mass in texture as shown in **Figure 5.11**. The explants thus retrieved were analyzed for mineralization and vascularization studies. The derived histological sections with Hematoxylin and Eosin staining showed a mixed morphological appearance and cellular organization (**Figure 5.13**) for both the explants. Larger part of the explant

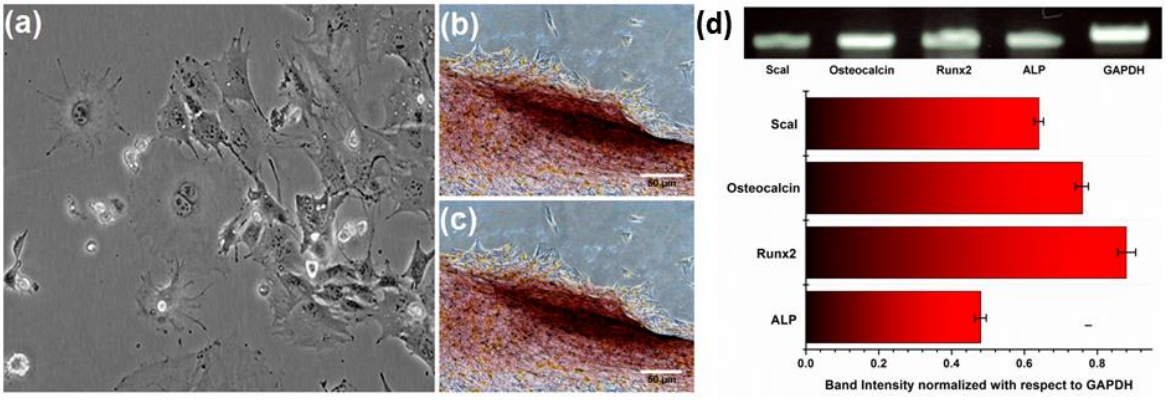

Figure 5.12. (a) Morphology of isolated murine osteoblasts cells viewed under microscope (magnification 10x); **(b)** and **(c)** Alizarin Red S staining of the isolated murine osteoblast cells (Scale bar represents 50 μm); **(d)** Histogram of RT-PCR data showing the gel electrophoretic bands for PCR products obtained from primer specific amplification of selected genes (drawn from the data obtained by band analysis).

was covered by osteoblasts indicating the fact that injectable bio-nanocomposite system is osteogenic in nature, which helps in its growth, proliferation and even in migration to an ectopic region. Certain areas of the explant showed the presence of calcium deposited mineralized zones for both the compositions with embedded mature osteoblasts like cells (osteocytes) characterized by their elongated nuclei. Apart from the mineralized zones, in few areas of the explants with injectate CDP-*f*-PU polymer along with murine osteoblasts showed the presence of thick mineralized granular (osteoid) structure with elongated nuclei.[30] This confirms the differentiation potential of osteoblasts into osteocytes and the mineralizing capability of osteoblasts in the vicinity of the bio-nanocomposite system. Additionally it also indicates the enhanced capability of mineralization and osteoid formation of CDP-*f*-PU loaded with osteoblasts. Numerous studies have shown that osteoblasts during bone formation process release various inflammatory cytokines, growth factors (such as growth factor β superfamily), bone morphogenetic protein as well as certain angiogenic factors.[31,32] The loaded osteoblasts in CDP-*f*-PU concerted the action of these factors and regulate the cellular proliferation, differentiation, recruitment of MSCs and preosteoblasts to the implant site as well as initiate angiogenesis to re-establish blood supply. In **Figure 5.13(iv)** blood vessels with red blood cells (stained intensely red) were seen in and around the osteoid like structures in osteoblast loaded CDP-*f*-

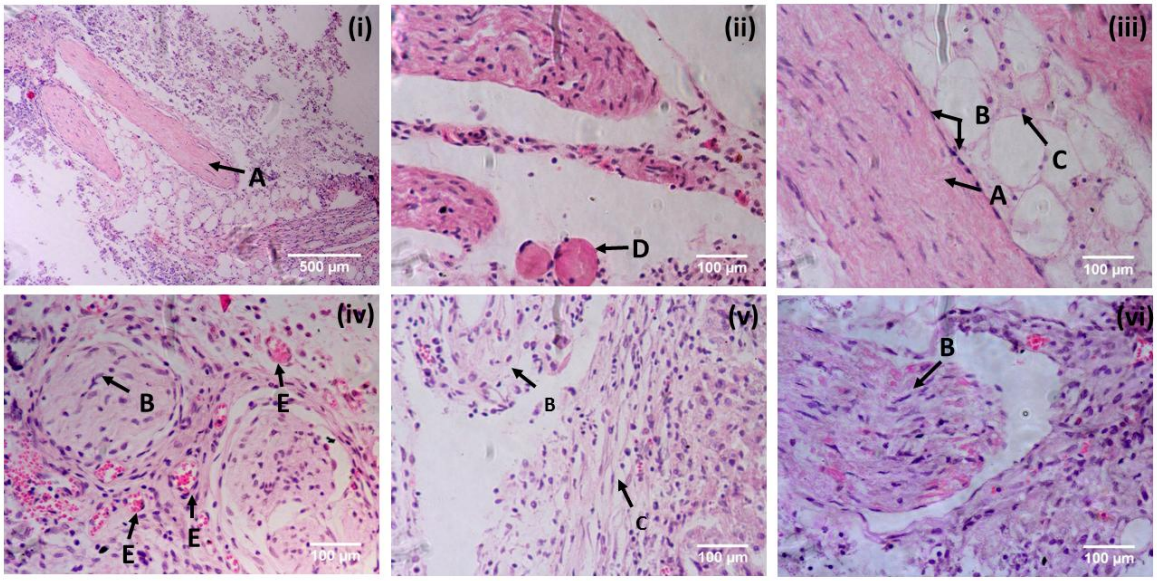

Figure 5.13. Representative histological sections of the extracted explant viewed under the microscope after Hematoxin and Eosin staining: Images **(i)** to **(iv)** represent CDP-*f*-PU with osteoblasts and images **(v)**, **(vi)** represent CDP-*f*-PU without osteoblasts. Image **(i)** is in 10x and **(ii)**, **(iii)**, **(iv)**, **(v)**, **(vi)** are in 40x magnification. Different zones are identified as A=Calcium deposited mineralized area, B=Osteocytes/Osteoblast embedded in the mineralized area, C=Fat cells, D=High calcium deposited mineralized granules and E=Vascular tissue/endothelial cells.

PU containing explants. This vascular cell organization indicates vascularization capability of the injectate. Further, Alizarin Red S assay was employed on the histological slides to visualize the mineralized nodules in the extracted explant (**Figure 5.14**). The results after phase-contrast microscopy showed the formation of multiple red colored spots throughout the tissue section. The red spots indicate the well-developed calcium nodules around osteoblasts and osteocytes, which were embedded within the heavily mineralized extra cellular matrix. The calcium deposition was found denser in polymer CDP-*f*-PU with loaded osteoblasts than the composition without cells. The fact that mineralization occur in an ectopic region proves the very osteogenic nature of the bio-nanocomposite. In order to ascertain the pattern of vascularization, a whole mount confocal microscopic study was performed (**Figure 5.15**). The micrographs revealed the presence of large numbers of oriented blood vessels in osteoblast loaded CDP-*f*-PU containing explant. The vessels in case of CDP-*f*-PU with osteoblasts were seen near the mineralized granular structure of the

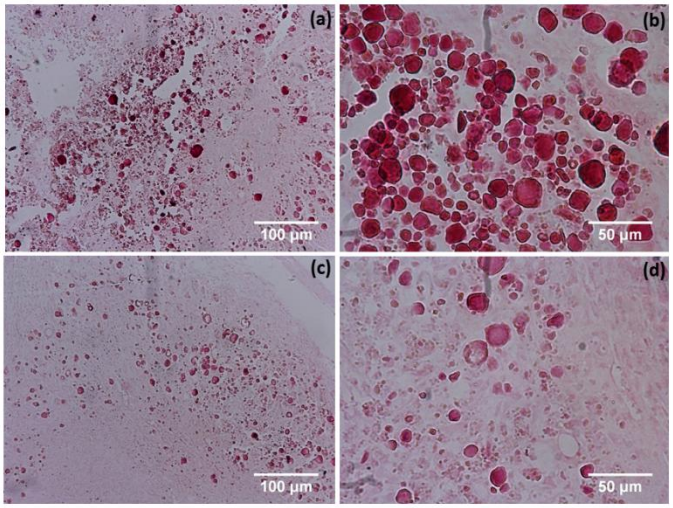

Figure 5.14. Alizarin Red S stained sections of explant from injectate CDP-*f*-PU (with osteoblasts): **(a)** at 10x and **(b)** at 40x; Alizarin Red S stained sections of explant from injectate CDP-*f*-PU (without osteoblasts): **(c)** at 10x and **(d)** at 40x.

explant indicating the occurrence of vascularization (**Figure 5.15a** and **b**). Presence of vasculogenesis was also found in case of CDP-*f*-PU injectate without osteoblasts, which were directed towards the patch of cells in the explant (**Figure 5.15c**). Thus, over all *in vivo* results clearly indicates the aptness of CDP-*f*-PU as a potent non-invasive biomaterial for bone tissue regeneration.

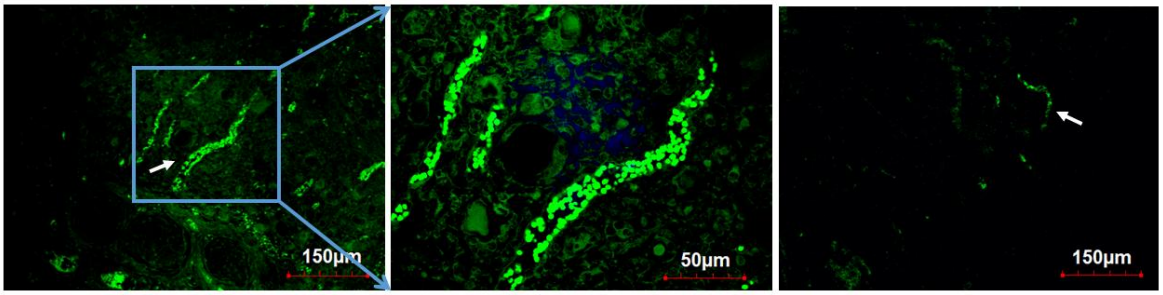

Figure 5.15. Whole mount confocal microscopic images of the explant containing CDP-*f*-PU as injectate (the freshly harvested explant shows a FITC (green) labeled anti-CD31 marking blood vessel lined endothelial cells): **(a)** 10x image of CDP-*f*-PU with osteoblasts showing presence of blood vessel near a mineralized granular structure (arrow marked) suggestive of vasculogenesis in the vicinity of calcified zone, **(b)** Image of CDP-*f*-PU with osteoblasts at 40x and **(c)** 10x image of CDP-*f*-PU without osteoblasts showing vascularization.

5.3.3.4. Biochemical profile and blood parameters

Biochemical analysis confirmed *in vivo* consequence of CDP-*f*-PU. The results of biochemical analysis are given in **Table 5.1** and **5.2**, respectively. The values of urea indicate normal kidney function and values were within the reference range. The safety value range of SGPT and SGOT (**Table 5.1**) addressed proper functioning of liver. However, compared to the control mice, the ALP level was found higher in the CDP-*f*-PU treated mice. Although elevated ALP is an indication of damaged liver during the bone formation/osteoblasts differentiation process, however, the scenario is different in the present case. The osteoblastic activity, including new bone formation, calcification and secretion of bone matrix resulted high level of this enzyme.[33] Increased ALP content marked the occurrence of bone formation. In the case of the control mice, the level of ALP remained constant. The haematological parameters of mice illustrated non-toxic and non-immunogenic responses of the host on exposure to CDP-*f*-PU (**Table 5.2**). The level of lymphocytes in the treated animal (with implanted materials) was determined in the peripheral blood of the host to ensure the biocompatibility and immunogenic nature of the implant material. From the results it was found that compared to the control mice, there was an increase in the levels of neutrophils and monocytes in the implanted mice due to the surgical wound. Although it did not surpass the reference limit. These observations thus suggest the safety aspect of the bio-nanocomposite in mice, as there was no inflammatory response was recorded on the CDP-*f*-PU treated groups throughout the experimental period. However, a sudden increment in the lymphocyte count was encountered in case of CDP-*f*-PU with osteoblasts treated cells. This might be due to the presence of osteoblast cells with the bio-nanocomposite, which might act as

Table 5.1. Biochemical profiles of control and CDP-*f*-PU treated male Swiss albino mice

Composition	ALP (405 nm) mUnit/mg of protein	Glucose	Urea	SGPT	SGOT
Control	156±4.1	93±2.5	68±2.3	55±1.5	92±2.8
CDP-*f*-PU (With OB)	215±3.6	85±3.0	61±1.5	58±2.0	101±2.0
CDP-*f*-PU (Without OB)	192±4.8	81±3.6	59±1.8	60±1.7	98±2.1

OB=Osteoblast

Table 5.2. Haematological parameters of control and CDP-*f*-PU treated male Swiss albino mice

Composition		Control		CDP-*f*-PU (with OB)		CDP-*f*-PU (without OB)	
		BE	AS	BE	AS	BE	AS
RBC (x 10^6/ µL) [Range-8.48-15.15]		7.35±0.5	7.32±0.4	6.96±1.1	7.42±0.2	7.22±0.8	7.54±0.70
WBC (x 10^3/ µL) [Range-9.1-28.7]		15.37±1.03	16.54±1.1	29.36±1.15	15.62±0.97	28.96±0.85	15.47±0.92
Differential %	**Neutrophils (%) [Range-9-34%]**	15.90±0.4	15.56±0.34	30.68±0.87	15.98±0.62	28.65±0.36	16.36±0.56
	Lymphocytes (%) [Range-65-85%]	65.59±1.6	66.68±2.0	81.36±2.26	63.56±1.45	77.91±1.75	64.16±1.89
	Eosinophils (%) [Range-0.5-3%]	1.68±0.1	1.33±0.15	1.66±0.18	1.16±0.21	1.87±0.13	1.24±0.01
	Monocytes (%) [Range-1-5%]	2.75±0.12	2.81±0.11	3.29±0.21	2.68±0.18	3.16±0.11	2.59±0.14

#BE=Before experiment, AS=After sacrifice, OB=Osteoblast

immunogenic to the host system. Although, the increase in the lymphocytes count was within the reference limit. Moreover, from the 1st to the 14th day, the implantation site was carefully observed for any post-implantation syndromes, *viz.*

fever, cardinal signs and rejection of the implant. Absence of these signs suggests its non-toxic and non-immunogenic behavior.

5.4. Conclusion

In summary, it is concluded that a multifunctional bio-nanocomposite of water dispersible hyperbranched polyurethane was developed by utilizing interdisciplinary knowledge of material science, bioscience and nanotechnology. Original waterborne hyperbranched polyurethane was made highly target specific by functionalizing with bio-nanohybrids of carbon dot with a panel of peptides, which stimulate osteoblast adhesion, proliferation and differentiation as well as induce vascularization. The study demonstrated cytocompatibility of carbon dot with human osteoblast. The findings are significant, which explore the viability of carbon dot as a nano-carrier for peptides for the first time. The sound mediated aqueous functionalization of the bio-nanohybrid with water dispersible polyurethane system provides a facile fabrication technique ensuring retention of bio-activity of the peptides. *In vitro* evaluation of osteoblast cell adhesion, proliferation and differentiation studies revealed the multifunctional nature of the hyperbranched polyurethane and thus endorsed the biocompatibility of the system for biomedical application. On functionalization with peptides, not only the biocompatibility was enhanced, but it also improved the osteoconductivity and the bone differentiation ability of the polymeric system. The enhanced adhesion, proliferation and differentiation of MG63 cells on the bio-nanocomposite thus endorsed the role of the bio-nanohybrid and biopolymer gelatin in bone healing process. On the other hand, mineralization and vascularization study showed the occurrence of calcification and blood vessel formation. The results of confocal and phase-contrast micrographs were implicative of osteogenic capacity of both osteoblasts laden and only polymeric system. In short, a unique carbon dot/peptide/polyurethane/gelatin system was successfully developed by a facile route, which could be directly applied for regeneration of bone tissues.

References

(1) Zhou, P., et al. Organic/inorganic composite membranes based on poly (L-lactic-co-glycolic acid) and mesoporous silica for effective bone tissue engineering, *ACS Appl. Mater. Interfaces* **6**, 20895--20903, 2014.

(2) Shalumon, K.T., et al. Modulation of bone-specific tissue regeneration by incorporating bone morphogenetic protein and controlling the shell thickness of silk fibroin/chitosan/nanohydroxyapatite core–shell nanofibrous membranes, *ACS Appl. Mater. Interfaces* **7**, 21170--21181, 2015.

(3) Li, L.L., et al. Biointerfaces: An adaptive biointerface from self-assembled functional peptides for tissue engineering, *Adv. Mater.* **27**, 3098--3098, 2015.

(4) Silva, D., et al. Synthesis and characterization of designed BMHP1-derived self-assembling peptides for tissue engineering applications, *Nanoscale* **5**, 704--718, 2013.

(5) Maude, S., et al. Synthesis and characterization of designed BMHP1-derived self-assembling peptides for tissue engineering applications, *Nanomedicine* **8**, 823--847, 2013.

(6) Jiang, H., & Xu, F.J. Biomolecule-functionalized polymer brushes, *Chem. Soc. Rev.* **42**, 3394--3426, 2013.

(7) Arica, M.Y., et al. Immobilization of laccase onto spacer-arm attached non-porous poly (GMA/EGDMA) beads: application for textile dye degradation, *Bioresour. Technol.* **100**, 665--669, 2009.

(8) Angenendt, P., et al. Toward optimized antibody microarrays: A comparison of current microarray support materials, *Anal. Biochem.* **309**, 253--260, 2002.

(9) Egusa, H., et al. Enhanced bone regeneration via multimodal actions of synthetic peptide SVVYGLR on osteoprogenitors and osteoclasts, *Biomaterials* **30**, 4676--4686, 2009.

(10) Horii, A., et al. Biological designer self-assembling peptide nanofiber scaffolds significantly enhance osteoblast proliferation, differentiation and 3-D migration, *PloS one* **2**, e190, 2007.

(11) Huttunen, M.M., et al. Long-term effects of tripeptide Ile-Pro-Pro on osteoblast differentiation in vitro, *J. Nutr. Biochem.* **19**, 708--715, 2008.

(12) Bergeron, E., et al. The evaluation of ectopic bone formation induced by delivery systems for bone morphogenetic protein-9 or its derived peptide, *Tissue Eng., Part A* **18**, 342--352, 2011.

(13) Wang, H., et al. Graphene oxide–peptide conjugate as an intracellular protease sensor for caspase-3 activation imaging in live cells, *Angew. Chem. Int. Edit.* **50**, 7065--7067, 2011.

(14) Das, B., et al. Bio-functionalized MWCNT/hyperbranched polyurethane bionanocomposite for bone regeneration, *Biomed. Mater.* **10**, 025011, 2015.

(15) Das, B., et al. Nanocomposites of bio-based hyperbranched polyurethane/funtionalized MWCNT as non-immunogenic, osteoconductive, biodegradable and biocompatible scaffolds in bone tissue engineering, *J. Mater. Chem. B* **1**, 4115--4126, 2013.

(16) Han, F., et al. Preparation, characteristics and assessment of a novel gelatin–chitosan sponge scaffold as skin tissue engineering material, *Int. J. Pharmacol.* **476**, 124--133, 2014.

(17) Gregory, C.A., et al. An Alizarin red-based assay of mineralization by adherent cells in culture: comparison with cetylpyridinium chloride extraction, *Anal. Biochem.* **329**, 77--84, 2004.

(18) Jørgensen, N.R., et al. Dexamethasone, BMP-2, and 1, 25-dihydroxyvitamin D enhance a more differentiated osteoblast phenotype: validation of an in vitro model for human bone marrow-derived primary osteoblasts, *Steroids* **69**, 219--226, 2004.

(19) Fischer, M.J. Amine coupling through EDC/NHS: A practical approach, in *Surface plasmon resonance: Methods and protocols*, N.J. Mol et al, eds., Humana Press**,** New York, 2010, 55-73.

(20) Mout, R., et al. Surface functionalization of nanoparticles for nanomedicine, *Chem. Soc. Rev.* **41**, 2539--2544, 2012.

(21) Kumada, Y., & Zhang, S. Significant type I and type III collagen production from human periodontal ligament fibroblasts in 3D peptide scaffolds without extra growth factors, *PloS One* **5**, e10305, 2010.

(22) Chun, J.S., et al. Differential translocation of protein kinase Cϵ during HeLa cell adhesion to a gelatin substratum, *J. Biol. Chem.* **271**, 13008--13012, 1996.

(23) Al-Nasiry, S., et al. The use of Alamar Blue assay for quantitative analysis of viability, migration and invasion of choriocarcinoma cells, *Hum. Reprod.* **22**, 1304--1309, 2007.

(24) Huttunen, M.M., et al. Effects of bioactive peptides isoleucine-proline-proline (IPP), valine-proline-proline (VPP) and leucine-lysine-proline (LKP) on gene expression of osteoblasts differentiated from human mesenchymal stem cells, *Br. J. Nutr.* **98**, 780--788, 2007.

(25) Murphy, G., et al. Purification and characterization of a bone metalloproteinase that degrades gelatin and types IV and V collagen, *Biochim. Biophys. Acta, Protein Struct. Mol. Enzymol.* **831**, 49--58, 1985.

(26) Komori, T. *Regulation of Osteoblast Differentiation by Runx2 in Osteoimmunology*, Springer, US, 2010.

(27) Nakamura, A., et al. Osteocalcin secretion as an early marker of in vitro osteogenic differentiation of rat mesenchymal stem cells, *Tissue Eng., Part C Methods* **15**, 169--180, 2009.

(28) zurNieden, N.I., et al. In vitro differentiation of embryonic stem cells into mineralized osteoblasts, *Differentiation* **71**, 18--27, 2003.

(29) Chitteti, B.R., et al. Hierarchical organization of osteoblasts reveals the significant role of CD166 in hematopoietic stem cell maintenance and function, *Bone* **54**, 58--67, 2013.

(30) Westendorf, J. J., et al. Wnt signaling in osteoblasts and bone diseases, *Gene* **341**, 19--39, 2004.

(31) Ai-Aql, Z.S., et al. Molecular mechanisms controlling bone formation during fracture healing and distraction osteogenesis, *J. Dent. Res.* **87**, 107--118, 2008.

(32) Gerstenfeld, L.C., et al. Fracture healing as a post-natal developmental process: Molecular, spatial, and temporal aspects of its regulation, *J. Cell. Biochem.* **88**, 873--884, 2003.

(33) Roudsari, J.M., & Mahjoub, S. Caspian Quantification and comparison of bone-specific alkaline phosphatase with two methods in normal and paget's specimens, *J. Intern. Med.* **3**, 478--83, 2012.